COMMUNICATION

Self-Glucose Feeding Hydrogels by Enzyme Empowered Degradation for 3D Cell Culture

Received 00th January 20xx,
Accepted 00th January 20xx

DOI: 10.1039/x0xx00000x

Mehrzad Zargarzadeh,[a] A. Sofia Silva,[a] Cláudia Nunes,[a,b] Manuel A. Coimbra,[b] Catarina A. Custódio*[a] and João F. Mano*[a]

Hydrogels have been used in combination with cells for several biomedical and biotechnological applications. Nevertheless, the use of bulk hydrogels has exhibited severe limitations in diffusion of oxygen, nutrients, and metabolites. Here, it is reported a support for cell culture where glucose is generated in situ by the own hydrogel degradation, allowing cell survival and function while promoting tissue growth. For this purpose, laminaran (or laminarin)-based hydrogels were fabricated immobilizing the adequate enzymes to obtain structural platforms for 3D cell culture and providing glucose feeding for metabolic activity of cells through polysaccharide degradation. We demonstrate that tumor A549 cells and human mesenchymal stem cells (hMSCs) can use the glucose resultant from the hydrogels degradation to survive and grow in non-added glucose cell culture medium. Additionally, *in-vivo* biocompatibility and biodegradability of laminaran-based hydrogels were explored for the first time. The self-feeding hydrogels exhibited high potential in cell's survival compared to native cell-laden laminaran hydrogels over two weeks of implantation. Such bioscaffolds with enzyme-empowered degradation capacity can be applied in diverse biotechnological contexts such as tissue regeneration devices, biofactories, disease models, and cell delivery systems.

Introduction

Tissue engineering (TE), as a multidisciplinary area, integrates engineering and biological principles to develop tissue/organ substitutes in case of failing or malfunctioning caused by an injury or disease. Such can be achieved through the combination of signalling molecules and cells in 3D biomaterial scaffolds with the capability of bearing cell infiltration and tissue organization.[1-3] Of the many bioscaffolds that have been applied in TE, hydrogels as hydrophilic cross-linked polymer networks, have gained significant attention due to their highly hydrated nature, leading to closely match the characteristics of biological tissues.[4-6]

Naturally derived hydrogels are an attractive 3D bioscaffolds for TE due to their high biocompatibility, inherent biodegradability, and crucial biological functions.[7-11] Laminaran (or laminarin, in its old designation) is a polysaccharide isolated from brown seaweeds comprised of (β1,3)-linked glucans with (β1,6) branches, containing hydroxyl groups that provide multiple conjugation sites for bioactive molecules.[12] This marine-derived polysaccharide has intrinsic properties that have established it as a promising biomaterial precursor.[13] Recently a toolbox of laminaran-based biomaterials was fabricated through the incorporation of various functional group.[14] Laminaran has been applied in the form of micro/nano platforms, namely photo-crosslinkable hydrogels and nanoparticles for biomedical applications.[15-17]

Remarkable achievements have been reported in the development of 3D constructs for cell culture, mainly on the control of the cell-materials interactions and on the mechanical and structural integrity of the matrix. However, considerable challenges remain unaddressed, such as the limited diffusion of nutrients, metabolites and oxygen, leading to the production of structures with restricted sizes and geometries, narrowing their applications.[18, 19] One of the proposed strategies to overcome these challenges is the development of technologies to pattern and control the organization of vascular cells via different mechanisms, including micropatterning, microfluidics, and 3D printing,[20-22] or through the assembly of micro-sized building blocks in bottom-up strategies.[23] Granting to the significant progress that has been achieved in fabrication of vascular networks for TE, current approaches still fail to reproduce their native organization. Therefore, novel scaffolds have been explored with the capability of providing sustained and controlled oxygen over time.[24] These oxygen-releasing biomaterials have been applied for cardiovascular TE, islet transplantation, wound healing, skin regeneration, and muscle regeneration.[25] Previous research was mainly done on the

[a] a. CICECO, University of Aveiro, Campus Universitário de Santiago, 3810-193 Aveiro, Portugal. Email: catarinacustodio@ua.pt, jmano@ua.pt.
[b] LAQV/REQUIMTE, Department of Chemistry, University of Aveiro, 3810-193 Aveiro, Portugal

oxygen's role in maintaining cells' viability due to its impact on modulating several critical cellular processes. It was demonstrated that human mesenchymal stem cell (hMSCs), in case of exposure to severe and long-term hypoxia, could survive and maintain their biological function if glucose supply is available.[26] Under anoxia (0.1% O2), hMSCs are unable to consume their exogenous energy sources and their survival exclusively revolve around anaerobic glycolysis. Since hMSCs are unable to adapt their metabolism to the lack of exogenous and reserved glucose, rapid deprivation of energy results in poor survival rate after implantation.[27] To the best of our knowledge, methodologies to provide the necessary amount of glucose, to ensure cells survival, have not yet been explored. Therefore, it is of interest to develop a glucose releasing scaffolds that could ensure cell survival by providing a sustained source of energy.

Considering the growing demands for biomaterials that can play multiple biological roles, as well as being capable of overcoming the current hurdles, we propose a radically innovative self-sustained 3D bioscaffolds for cell culture that take advantage of the degradation product (mainly glucose) of the laminaran hydrogels. The degradation mechanism of choice in this work is enzymatic which in comparison with other techniques, including acidic hydrolysis and gamma radiation, can favor the production of monomer product over oligomer, minimizing the potential for side reactions.[28] Endoenzymes have already been applied to hydrolyse laminaran, resulting in the production of oligosaccharides with a small amount of free glucose. [29, 30] However, recently, it was reported that the Bgl1B enzyme, an exo-β1,3-glucanase, could efficiently hydrolyse laminaran into glucose as a sole product.[30] Herein, we explore the degradation efficiency of laminarinase (endo-β1,3-glucanase) (LM) and glucoamylase (exo-α1,4-glucosidase) (GA) enzymes on various forms of the laminaran: low degree of methacrylation laminaran (LMeLam), high degree of methacrylation laminaran (HMeLam), and native polysaccharide. We hypothesize that degrading the non-reducing polysaccharide sugar units would result in direct glucose production without cleaving randomly the laminaran backbone chain. As a result, the glucose release would not have a significant impact on the hydrogel structural integrity. To have glucose autonomously accessible for feeding the cells, allowing them to carry out their metabolic and biological functions, enzymes were immobilized inside the laminaran hydrogel network (Figure 1). The fabricated hydrogels were characterized in terms of their mechanical properties, swelling and degradation capabilities. The biological performance of these novel self-feeding hydrogels was further evaluated *in vitro*. In addition, for the first-time biocompatibility and biodegradability of laminaran hydrogels were explored *in vivo*. The capability of the self-feeding hydrogels in cell's survival were also studied *in vivo*.

We believe, this is the first work reporting a self-sustained scaffold to successfully provide glucose to the cultured cells. Such innovation is expected to circumvent the limitations of the current hydrogel's strategies for cell culture and encapsulation that lack on nutrients diffusion and boosting the application of hydrogels in a variety of bioengineering applications including TE, fermentation, bioreactors biotechnology and cell expansion processes.

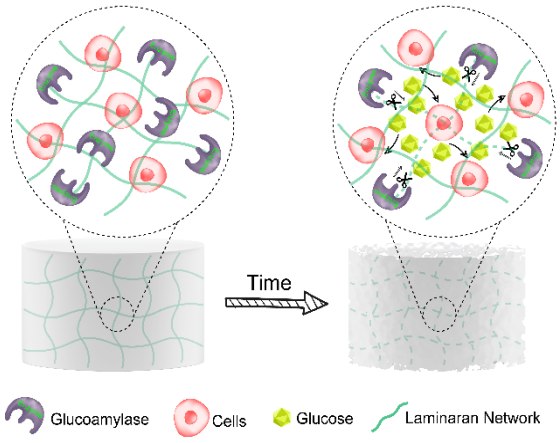

Figure 1.Schematic illustration of self-feeding hydrogels.

Results and discussion

Degradation studies of laminaran

Table 1 shows the efficiency of LM and GA enzymes in the hydrolysis of laminaran (not methacrylated) in terms of glucose production and evaluates the impact of the degree of methacrylation in the enzymatic hydrolysis. In line with previous studies, sugar analysis revealed that LM, as an endo-β-glucanase, hydrolysed laminaran mainly to oligosaccharides and barely to glucose(Figure S1a).[30] On the contrary, GA has shown a high efficiency in glucose production, as the main degradation product (Figure S1b). GA is extensively applied in the food industry to generate high glucose syrup and also in fermentation processes for the production of beer and ethanol.[31] We showed for the first time that GA can hydrolyse laminaran into high concentrations of glucose. The combination of the two enzymes have shown a decrease in the total glucose production (Table 1, Figure S1c). GA acts on polysaccharides more rapidly than on oligosaccharides[32] and since the combination of the two enzymes resulted in a chain length decrease due to the action of LM, GA activity was reduced and, consequently, glucose formation was decreased. A high degree of laminaran modification has shown a significant impact on enzymes activity when compared to the bare and LMeLam. This allows to infer that a high degree of hydroxyl groups substitution in laminaran results in hydrolysis inhibition of β1,6-linked side chains. Due to the ratio of the (β1,3) to (β1,6) linkages in laminaran (2.6 : 1)[33] and also the high activity of GA in both modified and bare form of laminaran, the hydrolysis of laminaran through GA seems to be by cleaving non-reducing sugar from both terminally-linked β1,3 and β1,6 linkages (Figure 2a). Considering these results, all subsequent analyses were performed using LMeLam and GA. An array of GA concentrations was tested to find out the conditions to produce glucose relatively close to the optimal glucose concentrations in the regular culture medium. After 14 days incubation of GA with

Table 1. Sugar analysis results from hydrolysis of different laminaran solutions after 4 days of incubation with enzyme(s).

Sample	Total harvested glucose (μmol)
Laminaran (10% w/v) + LM (21% v/v)	-
LMeLam (10% w/v) + LM (21% v/v)	-
HMeLam (10% w/v) + LM (21% v/v)	-
Laminaran (10% w/v) + GA (0.7% w/v)	4.16 ± 0.16
LMeLam (10% w/v) + GA (0.7% w/v)	2.96 ± 0.12
HMeLam (10% w/v) + GA (0.7% w/v)	1.63 ± 0.87
Laminaran (10% w/v) + GA (0.7% w/v) + LM (21% v/v)	3.05 ± 0.36
LMeLam (10% w/v) + GA (0.7% w/v) + LM (21% v/v)	1.61 ± 0.02
HMeLam (10% w/v) + GA (0.7% w/v) + LM (21% v/v)	0.07± 0.05

soluble LMeLam, 32% of LMeLam have converted to glucose unit by using 0.7% of enzyme, while 2% of enzyme showed a slight increase in the glucose obtained in comparison with 1.5%, being close to 58% conversion (Figure 2b). Therefore, for all further experiments, only 0.7 and 2% w/v of GA were used. After exploring the mechanism of degradation of soluble LMeLam, the degradation profile of LMeLam in hydrogel form (crosslinked) was examined. Results showed that the crosslinking of laminaran in the form of a robust gel did not significantly change the glucose production from the degradation of enzyme existing in solution (Figure 2c). Taken together, these results indicated that this degradation mechanism can be used as a glucose delivery platform for cell culture. In order to obtain an autonomous glucose releasing system, enzyme-immobilized hydrogels were further explored.

Characterization of enzymatically degradable hydrogel

To provide a self-sustained release of glucose readily accessible for cells, GA-encapsulated hydrogels were fabricated. The possible impact of GA entrapment on enzyme bioactivity was studied by measuring over time the produced glucose by GA-encapsulated hydrogels and comparing it to the produced glucose by enzymatic hydrolysis of LMeLam solution using the free enzyme. The sugar analysis results of GA-encapsulated hydrogels have demonstrated that conversion to glucose unit was reduced when compared to free enzyme degradation of LMeLam in solution as well as laminaran hydrogel degradation from outside (Figure 2d, Figure S2). This appears to be a case of the enzyme orientation during the immobilization which could have enzyme active site not accessible for laminaran.[34] Besides monosaccharides (glucose), disaccharide and trisaccharide were also produced through degradation of the GA-encapsulated hydrogels (Table S1). We believe these by-products will not have any impact on cell's viability, due to their negligible quantities.

Within 24h, 10% and 23% of enzyme were leach out from 0.7% and 2% enzyme encapsulated hydrogels, respectively (Figure S3). This burst release is probably attributed to the excessive amount of enzyme close to the surface of the hydrogels. After long term incubation of these hydrogels in PBS (28 days), no signs of extra leakage were observed, which indicates high stability of hydrogels in terms of entrapping the enzyme. The influence of the incorporation of different enzyme concentrations on the microstructure of the hydrogel was investigated by cryo-SEM. Representative images of the analysed cross sections are depicted in Figure 3a. Immobilizing GA in the laminaran hydrogels resulted in an open structure with significantly higher pore sizes over time, peaking for the formulation encapsulating 2% GA in both time points (Figure 3b). This enhancement would have an important role in improving cell proliferation and mass transport in 3D structures, particularly in hydrogels.[35] Compressive stress-strain curves of the self-degradable hydrogels and native laminaran hydrogels from day 0 to day 14 (from left to right) are shown in Figure S4. At day 7 and 14, maximum compressive stress and ultimate strain were both significantly decreased in both formulation of GA-encapsulated hydrogels when compared to the native laminaran hydrogels. Changes were also found in stiffness, as shown in Figure 3c. No significant difference was found in the young modulus of native hydrogels over 14 days (approximately 23 kPa). GA encapsulated and native hydrogels have demonstrated similar elastic modulus immediately after fabrication (day 0). However, after 14 days the elastic modulus was decreased significantly from 22.8 ±0.9 kPa to 12.8 ± 0.5 kPa and from 24.1 ± 1.9 kPa to 9.0 ± 2.0 kPa, for 0.7% and 2% in GA-encapsulated hydrogels, respectively. This confirms the impact of the enzyme along time and the consequent decay on the mechanical properties of the hydrogels after 2 weeks. These findings are in agreement with the porosity results, confirming the correlation between pore size and the evolution of the mechanical behaviour.[36, 37]

By visual observation, the degradation is clearly obvious in GA-encapsulated hydrogels over 14 days in both swollen and dry forms (Figure 3d). However, the hydrogels maintained their structural integrity and handleability. The degradation of the hydrogels was also monitored by the weight changes (Figure 3e,f). Native laminaran hydrogels and GA-encapsulated hydrogels had relatively similar initial wet and dry weight (30 min after crosslinking). Hydrogels containing GA continued to increase up to about 23% of their initial wet weight through one week, which corresponded to the degradation and boost in water uptake due to higher pores size. After two weeks, the degradation was sufficiently substantial to observe an effective loss of mass. Native laminaran hydrogels exhibited bulk swelling without any apparent dissolution over 14 days, indicating long term stability.[17] The same profile of wet weight changes was reported in enzymatically-degradable peptide-crosslinked alginate hydrogels, where hydrogels initially exhibited an increase in wet weight due to the swelling and eventually dissolution as a result of more pronounced degradation.[38] After 7 days, the dry weight of GA-encapsulated hydrogels in both formulations started to significantly decrease when compared to the native laminaran hydrogels (Figure 3f), indicating a dissolution and mass loss, which confirms the

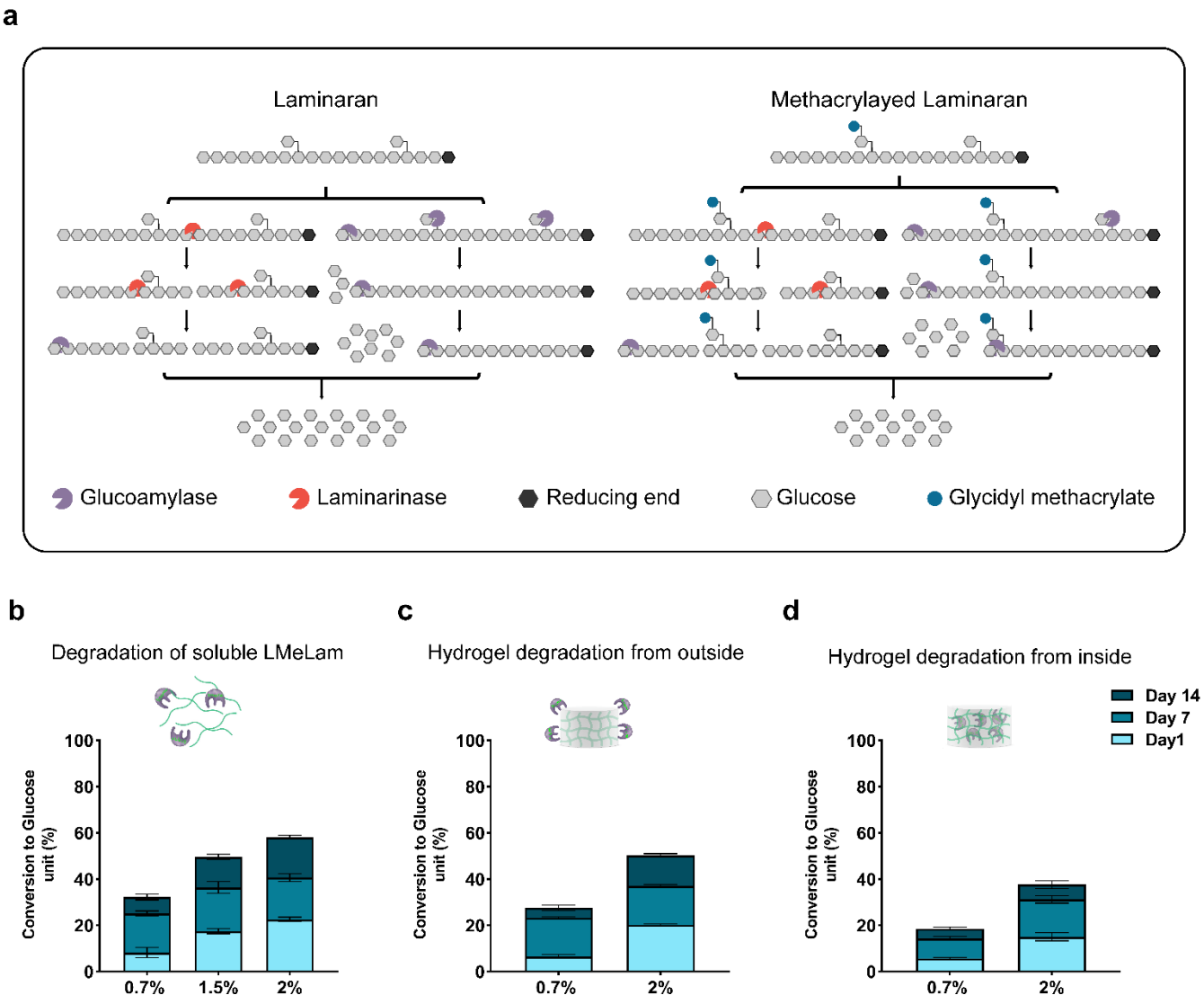

Fig 2. Enzymatic degradation of various forms of laminaran. a.GA and LM activities on bare and modified laminaran structures: LM hydrolyses randomly the (β1,3)-linked glucans and GA hydrolyses non-reducing end of (β1,3)-linked glucans and (β1,6) branches of laminaran. Percentage of Methacrylated laminaran converted to glucose unit via degradation (considering the average degree of substitution~30): b. LMeLam in solution; c. Cross-linked (gel form) by incubation with different concentrations of GA concentrations; d. GA-encapsulated (0.7 and 2% w/v) laminaran hydrogels. Data are expressed as mean ± SD (n = 3).

degradation profile and supports the reduction of wet weight. However, no effective loss of mass was observed up to 3 days. While native laminaran hydrogels maintained their dry weight over two weeks, GA-encapsulated hydrogels lost approximately 12% and 20% of weight for 0.7% and 2% formulations, respectively.

Evaluation of laminaran hydrogel degradation for supporting cells growth

To validate that cells could effectively use the glucose obtained from the degradation of hydrogels to grow and maintain their metabolic activity, cells seeded in glucose free medium were placed in contact with laminaran hydrogels and GA (Figure 4a). As such, any difference in cells response could then be attributed directly to the glucose released from the degradation of hydrogels.

Cancer cells are characterized by having high level of glucose consumption. In case of glucose starvation their proliferation would dramatically be reduced.[39] Therefore, human adenocarcinoma alveolar basal epithelial (A549) cells were initially used to test the potential of glucose resultant from hydrogels degradation as a glucose alternative in culture medium. Mesenchymal stem cells (MSCs) were also used to test the ability of degrading hydrogels to support the culture of human-derived stem cells. In the absence of enzyme, A549 cells exhibited rounded shape morphology, while spread cell morphology was evidenced in the presence of the enzyme (Figure 4b). The positive effects of glucose production due to enzymatic degradation on A549 cells was also observed through analysis of the metabolic activity (Figure 4c). Overall, in presence of the hydrogels and GA in the medium, cells have shown high viability (more than 60%) over two weeks,

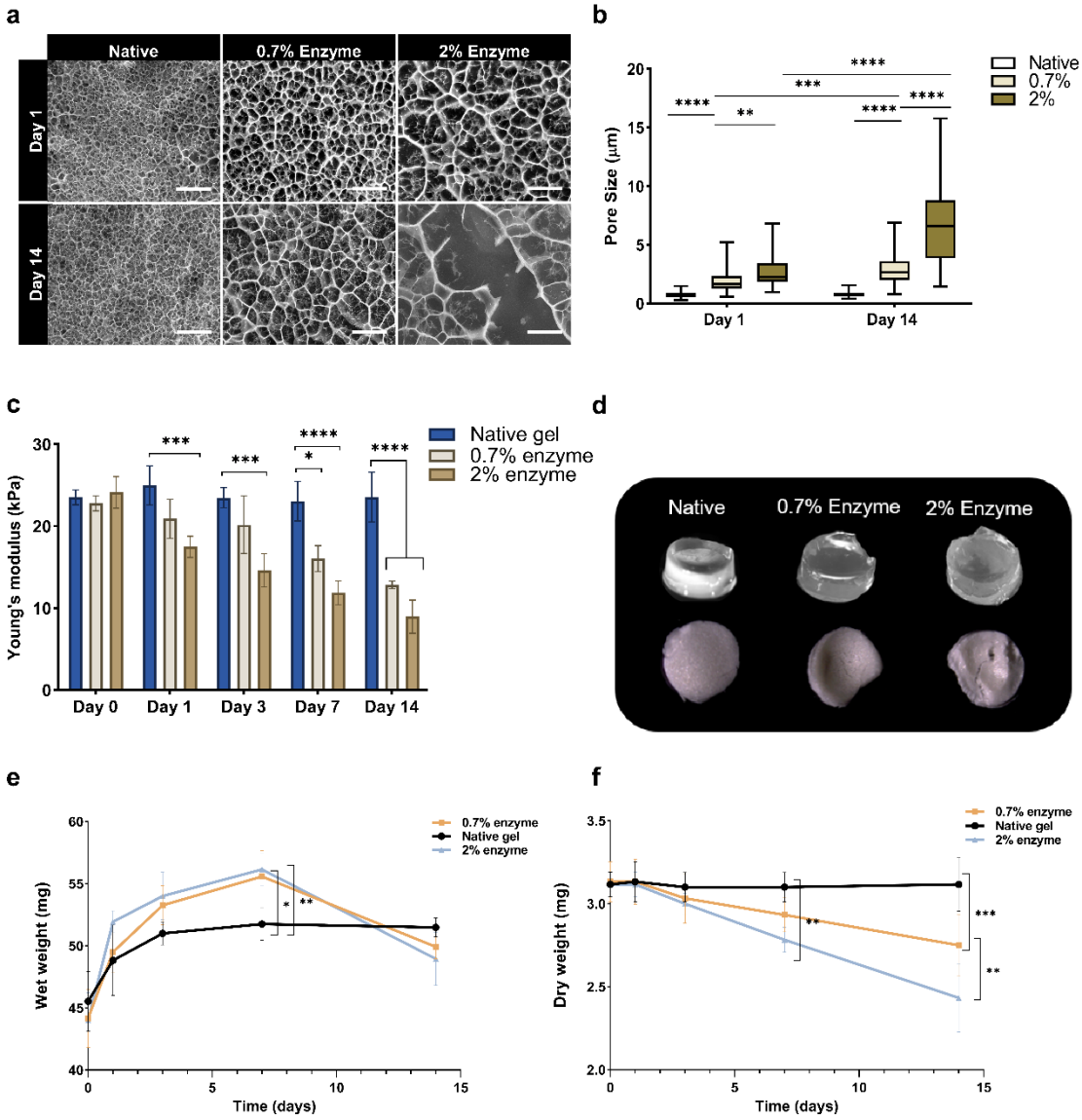

Fig 3. Characterization of GA-encapsulated laminaran hydrogels. a Cross-sectional cryo-SEM micrographs of enzyme (0.7 and 2%) encapsulated and native laminaran hydrogels. Magnification 5000x (scale bar 5 µm). b Pore size distribution of GA-encapsulated and native hydrogels for day 1 and day 14. c Young's modulus of the fabricated hydrogels over time (n=3). d Images of native and enzyme encapsulated hydrogels in wet (up) and dry (down) form after 14 days incubation in PBS. Wet weight (e) and Dry weight (f) changes of enzyme encapsulated (0.7 and 2% (w/v)) and native hydrogels up to two weeks (n=6). Error bars indicate ± standard deviation. *P < 0.05, **P < 0.01 , ***P < 0.001 and ****P < 0.0001. # Significantly different from all the others on the right.

indicating that the degradation of the laminaran hydrogel has provided sufficient glucose for cells to maintain their metabolic activity. In contrast, the absence of enzyme has shown significant reduction of their viability, possibly due to glucose deprivation. MSCs in presence of enzyme had spread over 14 days and maintained alive, whereas cells in absence of enzyme and, consequently, with no available glucose, underwent morphological changes, beginning to round up in day 1. Over 14 days most of the cells died and detached from the surface (Figure 4d). MSCs presented significantly higher viability in the presence of enzyme, in both concentrations, compared to the condition without enzyme in all timepoints. This indicates that stem cells were successfully adapted to grow through using glucose from the degradation of the laminaran hydrogel.

3D Encapsulation in self-feeding laminaran hydrogel

Encapsulated cells were homogeneously distributed through the hydrogels (Figure 5a,c). Live/dead staining demonstrated that most of the encapsulated cells remained viable in all the hydrogel formulations (~≥90% viability) indicating that GA had no cytotoxic effects. More importantly, enzymatic degradation provided sustained release of glucose over 14 days to maintain the cells viable (Figure 5a,c). In contrast, cells in native laminaran hydrogel were mostly dead, as expected due to absence of glucose. Higher viability was found for both cells in hydrogels containing enzyme when compared to positive control (Figure 5b,d). This availability of glucose for cells yielded higher metabolic activity. Moreover, degradation of laminaran had expanded the space available for cells to proliferate and

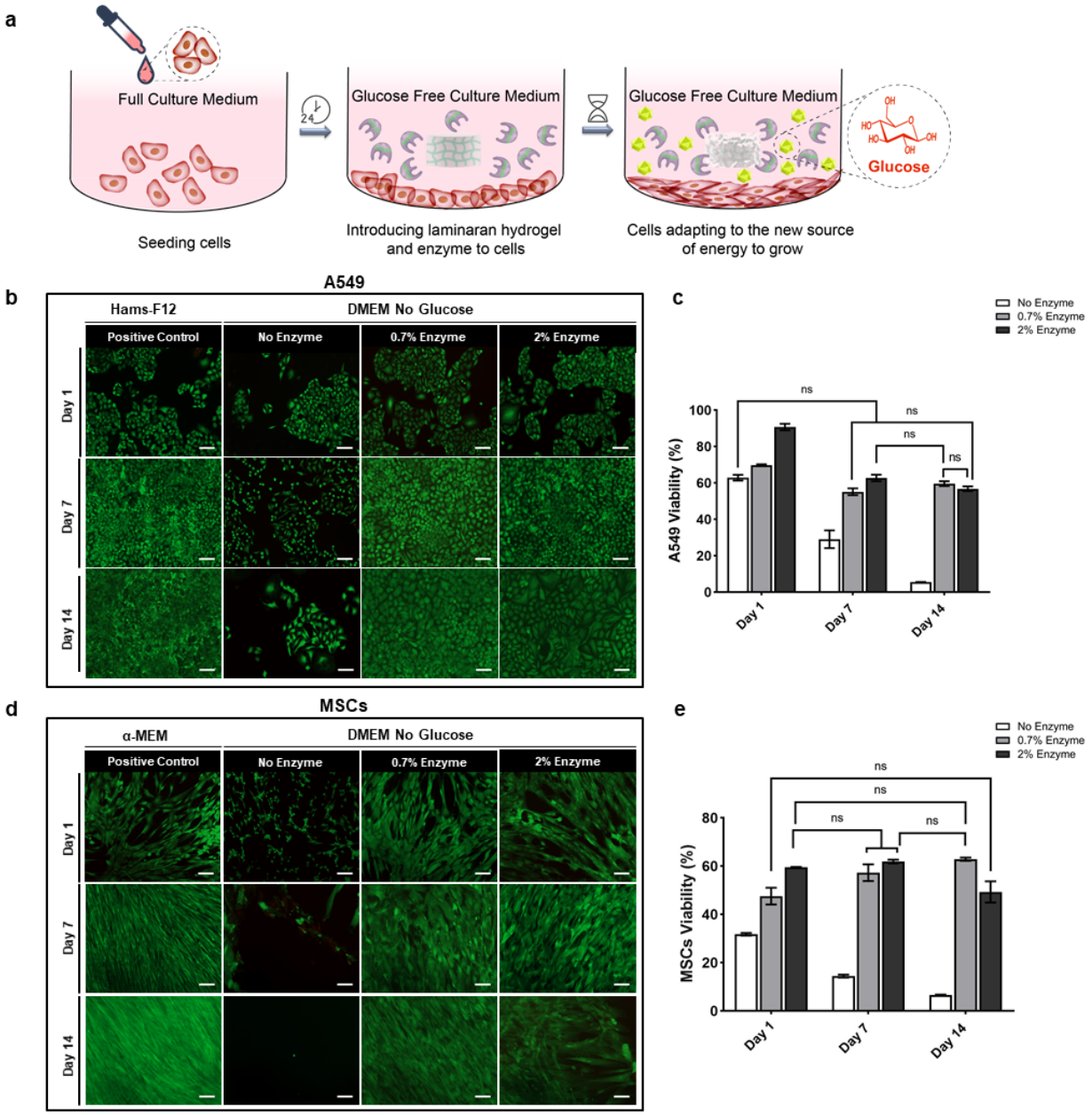

Figure 4. Evaluation of cells response in laminaran hydrogels. a. Schematic illustration of the process to evaluate cells response to glucose replacement. Representative fluorescence microscopy images of live/dead assay for b. A549 and d. MSCs adapted to glucose replacement in cell culture medium. Metabolic activity of c. A549 and e MSCs at 1, 7, and 14 days of cell culture. Scale bar=100µm. NS indicates no significant difference.

maintain their metabolic activity over time. Viability reduction of MSCs in 2% enzyme hydrogel over 14 days might be an indication of glucotoxicity due to the detrimental effects of high glucose concentration. In a further study, viability of encapsulated cells (both A549 and MSCs) was assessed over two weeks of culture, in glucose free medium through live-dead assay (Figure S5) where there was no available glucose or glucose was provided from inside or outside, via degradation. In the case of no available glucose, both cell lines died in both periphery and core of the hydrogels (Figure S5.1). Cells in the periphery of the hydrogels were maintained alive due to their access to the generated glucose from outside degradation of hydrogels (Figure S5.2), while inner cells mostly died due to the limited access to glucose. GA-encapsulated hydrogels (0.7%) have clearly demonstrated high viability in both periphery and core of the hydrogels indicating autonomous accessibility of glucose for cells in the whole hydrogel (Figure S5.3). Cells proliferation assays were performed by DNA quantification. A549 as well as MSCs were able to proliferate inside the enzyme encapsulated hydrogels, as can be seen by the increase in DNA content (Figure 5e,f) over 14 days of culture, while no differences were observed in the absence of enzyme for both cell lines. DNA content for 2% GA was maintained constant from day 7 to day 14 which indicates there was no proliferation.

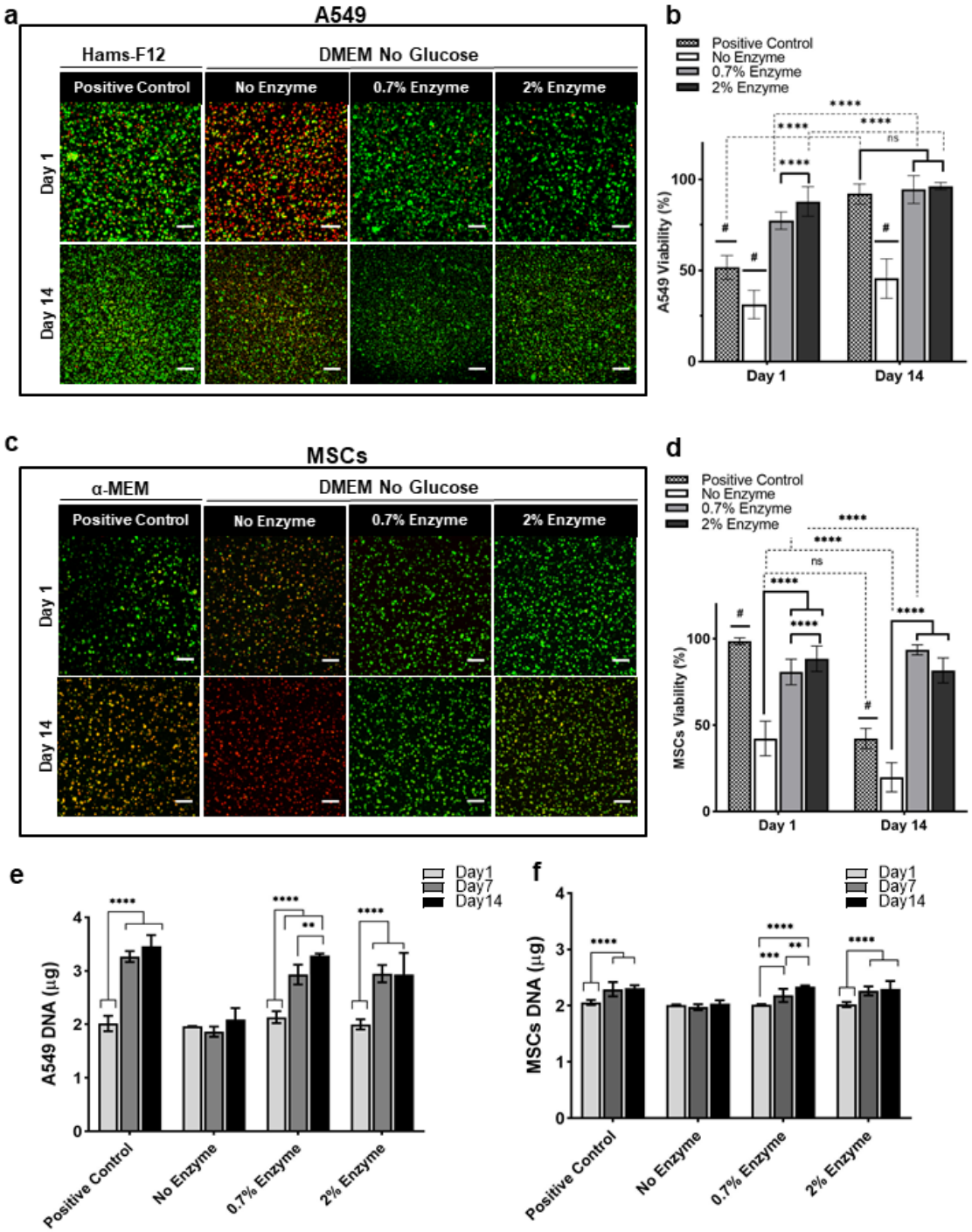

Figure 5. Cytotoxicity and cell proliferation upon encapsulation in laminaran hydrogels. Live/Dead fluorescent staining of 3D encapsulation of a.A549, c. MSCs hydrogels. Cell viability (%) of b A549 and d MSCs over two weeks. DNA results of e A549 and f MSCs at 1, 7, and 14 days of cell culture. Scalebar=100µm. Bars indicate mean ± standard deviation. $p < 0.05$: *$p < 0.05$; **$p < 0.01$; ***$p < 0.001$; ****$p < 0.0001$. # Significantly different from all the others on the right. Scaling bars are 100µm.

Viability in self-feeding laminaran hydrogels was quantified using z-stack images by counting live and dead cells. The reduction in viability of MSCs by day 14 in 2% GA-encapsulated hydrogel was due to the increase in the number of cells entering apoptosis phase (stained with PI). Since PI binds to DNA, it confirms the presence of DNA of cells in the hydrogel. Accordingly, the DNA content of day 14 maintained the same as day 7 although viability have decreased due to high glucose concentration. In order to investigate that glucose production rate, meet with the cellular glucose consumption rate, we plotted glucose consumption (approximately 9.2pmol/cell/day[40]) vs glucose production in self-feeding hydrogels (figure S6). As it is shown in the results, 0.7% enzyme in 24h produced almost the same quantity of glucose which cells would require to consume. In the case of 2% GA since the beginning, significantly higher quantity of glucose has been produced which led to the glucotoxicity. This is in agreement with viability reduction of MSCs by day 14 (Fig 5d) and the stopping of proliferation for 2% GA from day 7 to day 14 (Figure 5f). These results prove the ability of self-feeding hydrogels for

long-term cell function, overcoming a major challenge for TE strategies.

***In-vivo* animal studies**

To demonstrate the practical ability of such hydrogels, *in-vivo* experiments have been performed on nude mice through subcutaneously implantation of three different groups of hydrogels. For testing self-feeding hydrogels *in-vivo*, 0.7% GA condition was selected due to their better in-vitro performance compared to 2% GA. The experimental design is shown in Figure 6.a. Hydrogels (n=2/mice) were subcutaneously implanted (Figure 6.b) and explanted after 7 and 14 days (Figure S7). No significant differences in variability were found between female and male groups in all the performed experiments. The body weights of mice did not change over one week (Figure S7.b) and two weeks (Figure S7.c) in all the tested group which is a good indicator of no acute toxicity in the implanted materials. We evaluated the degradation of laminaran-based hydrogels using 2D ultrasound imaging over time (Figure 6.c). Obvious changes in the size of GA-encapsulated hydrogels clearly confirmed enzymatic degradation over 14 days of implantation while cell-laden hydrogels and blank laminaran hydrogels were completely intact without any sign of degradation (Figure 6.d). These results are in line with previous studies presenting that there is no existing enzyme secreted by the saliva glands, pancreas and gastrointestinal tract in mammals that can hydrolyse β(1–3) and β(1–6) linkages of laminaran.[41] In order to assess cell's survival *in-vivo*, live-dead assay was performed. Subsequently, the hydrogels were explanted at day 7 and day 14 and after cutting the edges of the hydrogels by sharp razor blade, thin slices of the hydrogels were promptly stained (Figure 6.e). MSCs have manifested a high level of viability (in the central region of the 0.7% enzyme encapsulated hydrogels) after 7 and 14 days of implantation while in the absence of GA, cells were mostly dead (Figure 6.f). In the case of the blank hydrogels no cells were detected in the hydrogels (Figure 6.e). These findings highlight the capability of such self-feeding hydrogels to provide glucose as the most important substrate of cell metabolism, in the *in-vivo* conditions where cells are exposed to the limited supply of oxygen/nutrients. Local tissue response to the implanted hydrogels was characterized through the histological assessment (H&E staining) following the ISO-10993-6[42] inflammatory-reaction intensity guidelines: minimal or no reaction < slight < moderate < severe. As it is shown in Figure 7, all the implanted hydrogels caused inflammatory reaction at day 7 which was reduced by day 14 of post implantation. Most of the population of inflammatory cells were consisted of polymorphonuclear cells (PMNs) and macrophages. Table 2 summarizes scores of inflammatory responses of the implanted hydrogels based on the ISO-10993-6. Self-feeding hydrogels (0.7%) have presented a low inflammatory intensity (slight reaction) over two weeks. Supplementary Table S2 and S3 lists the scoring data for all the conditions including the control for day7 and day 14 in detail.

Conclusions

In this study, self-feeding hydrogels were fabricated by immobilizing specific enzyme through a facile method using minimal elements. GA was presented for the first time to hydrolyse laminaran into high concentrations of glucose. We demonstrated that native and enzyme encapsulated hydrogels had the same initial mechanical properties but different and tuneable degradation kinetics thereafter. Increasing the GA concentration in the hydrogels led to a decrease of elastic modulus, ultimate strain and ultimate stress when compared to native laminaran hydrogels, as the average porosity for the same conditions was increased over time.

Higher GA concentration induced higher pore size and provided larger contact surface area between the hydrogel and media. This resulted in higher water content compared to the native hydrogels in 7 days and afterwards faced to the dissolution and mass loss. Moreover, tracking the degradation via changes in dry weight of the hydrogels revealed that the kinetics of this process is an enzyme concentration dependent manner. *In vitro* studies of this self-feeding hydrogel have demonstrated significantly high viability of the encapsulated MSCs and A549 cells in glucose free culture medium, attributed to the sustained release of glucose resultant from enzymatic degradation of the hydrogel. Furthermore, higher pore size induced by degradation resulted in expanding the available space for cells and eventually, improved their access to oxygen and other nutrients during the culture. Such process should be consistent with the higher proliferation ability of the cells in LMeLam hydrogels with GA. Furthermore, *in-vivo* biocompatibility and biodegradability of such self-sustained hydrogels highlights its promise for further use in biomedical applications.

Our novel self-degradable hydrogel can serve as a 3D scaffold for cells while providing a sustainable nutrition source through gradual release of glucose over time, a concept never explored before. It is noteworthy to address that any other glucose-based polymer may potentially be replaced in such system. In conclusion, these results, combined to the fact that most current bioscaffolds suffer from lack of nutrient diffusion, clearly suggest the potential of this hydrogel in future developments of 3D structures in a wide range of biotechnological applications as an autonomous cell supporting system. This self-maintained and biocompatible material could potentially be used as a closed culture system for living cells and any other microorganisms, as a novel platform for cell delivery, or to be used in bioreactors.

Experimental

Degradation studies of laminaran solution

To find out the mechanism behind laminaran degradation, initial degradation assays were performed on bare (not modified) and methacrylated laminaran (MeLam) solutions. Synthesis of the MeLam was carried out by reacting glycidyl methacrylate (Acros Organics) with laminaran (Carbosynth)

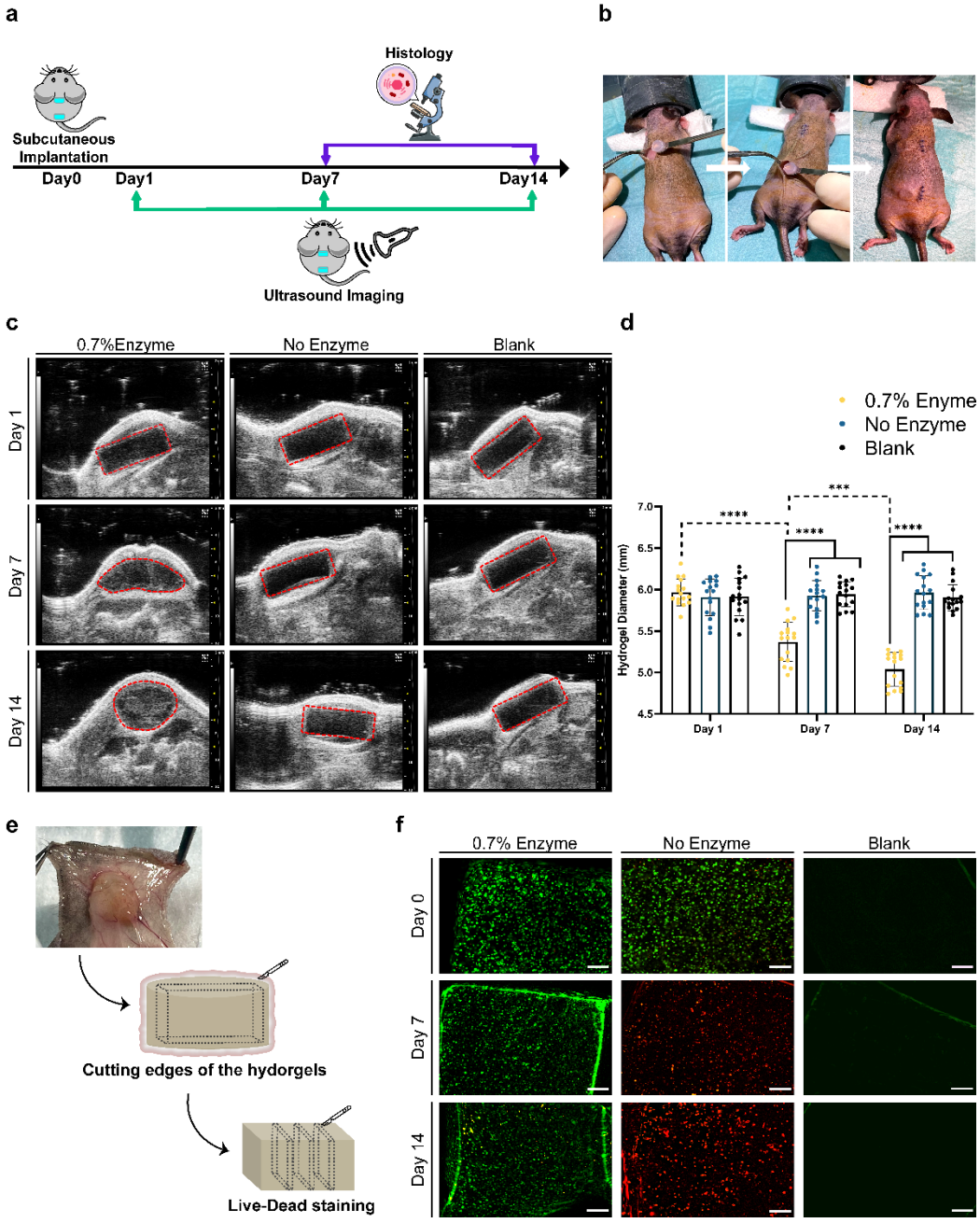

Figure 6. In-vivo-evaluation of three groups of laminaran-based hydrogels implanted in nude mice: self-feeding hydrogels (encapsulating MSCs with 0.7% GA), native cell-laden laminaran hydrogels (encapsulating MSCs without enzyme) and blank hydrogels (without cells and enzyme). a. Schematic representation of the in-vivo experimental design. b. surgical procedure for implanting two hydrogels per mice. Representative results of subcutaneous implantation of laminaran-based hydrogels in nude mice from both sexes c) Ultrasound images of the implants at day 1,7 and 14. d) Quantitative plotting of hydrogel diameter over two weeks of implantation. e) Schematic presentation of live-dead staining process of the explanted hydrogels. f) Representative fluorescence microscopy images of live/dead staining at day 0 (implantation day), 7 and 14, where the green stain represents the live cells, and the red stain represents dead cells. Scale bar=200µm. Bars indicate mean ± standard deviation. $p < 0.05$: *$p < 0.05$; **$p < 0.01$; ***$p < 0.001$; ****$p < 0.0001$.

based on a previously reported protocol. [17] In brief, laminaran (1 g) and 4-(N,N-dimethylamino)pyridine (DMAP;167 mg; Acros Organic) were dissolved in 10 mL of dimethyl sulfoxide (DMSO; Sigma-Aldrich) under nitrogen atmosphere. LMeLam and HMeLam were obtained by adding 2.9 × 10−3 and 5.1 × 10-3 mol of glycidyl methacrylate, respectively. The reaction was run at room temperature (RT) for 48 h in dark, then stopped by adding HCl solution (37%) (Sigma-Aldrich) to neutralize DMAP. After dialysis (benzoylated membrane; 2000 MWCO; Sigma-Aldrich) for 7 days against distilled water, the purified solution was freeze-dried. Enzymatic hydrolysis was performed by incubating endo (laminaranase 16A (Nzytech)) and exo-enzymes (glucoamylase from Rhizopus (TCI)), individually or in combination of both, with different laminaran solutions. LMeLam, HMeLam and bare laminaran (10% w/v) were incubated individually with enzyme(s) in a phosphate buffered saline (PBS, Sigma-Aldrich; pH 7.4) solution at 37°C. To monitor the degradation products, in particularly the glucose concentration, sugar analysis was performed based on the reported technique and quantified using 2-deoxyglucose as an

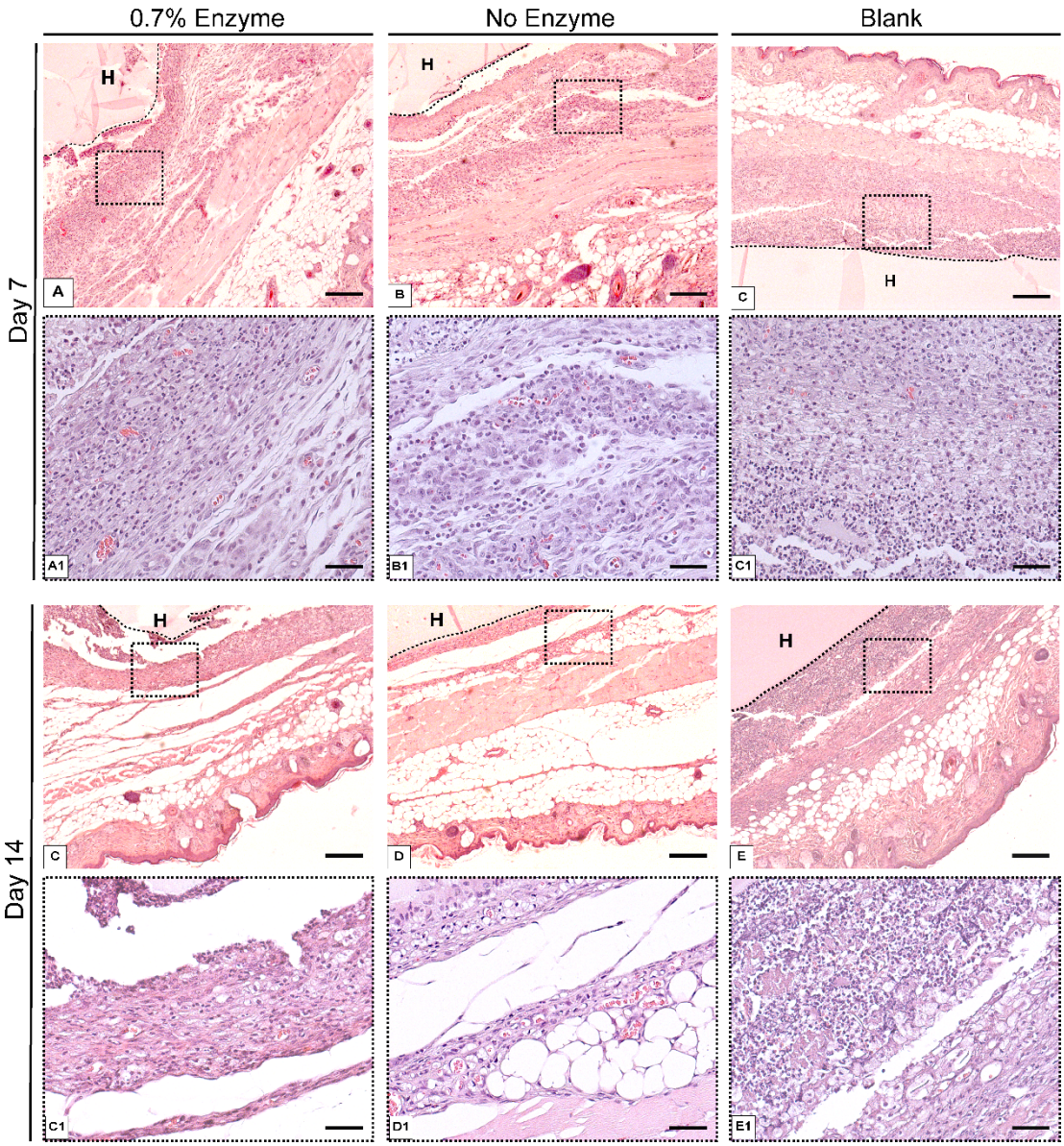

Figure 7. Histological analysis of subcutaneous implanted hydrogels and surrounding tissue. Representative haematoxylin and eosin-stained (h&E) sections of the implants with surrounding tissue at day 7 and day 14 post implantation. Low magnification images are provided in the upper panels (A-E), scale bars: 200 µm, while higher magnification images are in the lower panels (A1-E1), scale bars: 50 µm.

internal standard[19]. At each time point, samples were reduced with NaBH4 (15% in NH3 3 M, 1 h, 30°C) and further acetylated with acetic anhydride (3 mL), in the presence of 1-methylimidazole (450 µL), at 30 ºC during 30 min. Liquid-liquid extraction method was applied to separate alditol acetates using dichloromethane. Finally, after evaporation of the organic solvent, samples were solubilized in anhydrous acetone and analysed by Gas Chromatography using a Mass Spectrometry detector (GC-MS) or Gas Chromatography using a Flame Ionization Detector (GC-FID).

Degradation of laminaran hydrogel

(w/v) with 0.5% (w/v) of 2-hydroxy-4-(2-hydroxyethoxy)-2-methylpropiophenone (Irgacure 2959) (Sigma-Aldrich). Hydrogels were formed by pipetting 40 µL of polymer solution to polydimethylsiloxane (PDMS) cylindrical molds with a diameter of 6 mm followed by UV irradiation at 2–3 W/cm^2 for 120 s. The glucose production from hydrogels degradation was measured over 14 days through sugar analysis while hydrogels (n=3) were incubated in GA enzyme solution (0.7%, 2% w/v) at 37°C. Sugar analysis was performed as stated in previous section.

The hydrogel precursor solution was prepared by dissolving lyophilized LMeLam in PBS at the final concentration of 10%

Fabrication of enzyme-encapsulated laminaran hydrogels: Enzyme encapsulated laminaran hydrogels were fabricated to obtain sustained degradation and consequently, a gradual production of glucose over time. After ensuring complete dissolving of the photoinitiator (0.5% w/v) and LMeLam (10%) in PBS, GA enzyme was then added to the mixture at final concentrations of 0.7% and 2% w/v.

Table 2.Inflammatory response of the implanted hydrogels according to ISO-10993-6 classification. Scale range of 0.0-2.0 = minimal or no reaction, 3.0-8.9 = slight reaction, 9.0-15.0 = moderate reaction, >15.0= severe reactions.

Day 7			
Condition	**Average Score**	**Final Score**	**ISO Classification**
Control	10.54 ± 2.12		
Blank	20.41 ± 0.99	9.92	**Moderate reaction**
No Enzyme	18.16 ± 0.72	7.67	**Slight reaction**
0.7% Enzyme	18.83 ± 0.89	8.33	**Slight reaction**
Day 14			
Control	13.00 ± 2.12		
Blank	16.42 ± 1.04	3.41	**Slight reaction**
No Enzyme	14.25 ± 1.11	1.25	**Minimal or No reaction**
0.7% Enzyme	17.58 ± 0.26	4.58	**Slight reaction**

After thorough mixing, the resulting solution (40 µL) was pipetted to cylindrical PDMS molds and afterwards irradiated by UV for 2 min.

Characterization of the enzymatically degradable hydrogels

To investigate the impact of the enzyme entrapment on its bioactivity, the glucose produced by enzyme encapsulated hydrogels was measured through sugar analysis. At determined time points, hydrogels were physically destroyed to quantify the encapsulated/released glucose. The samples were then centrifuged for 5 min at 500g at RT and the amount of sugar in the supernatant was analysed using sugar analysis. Glucose concentration measured from the hydrolysis of LMeLam solution by GA was counted as 100%. The ability of the hydrogels to retain the incorporated enzyme was determined by immersing enzyme-encapsulated hydrogels (n=8) in PBS at 37°C for 28 days. Protein content in solution was further quantified by using the Pierce Micro BCA Protein Assay Kit. The cumulative release of GA from each hydrogel was calculated as follows:

$$\text{Cumulative Release (\%)} = Mt/M0 \times 100\%$$

where M0 is the amount of enzyme preloaded into hydrogel and Mt is the total amount of enzyme leached from the hydrogel at time t.

Native laminaran and enzyme encapsulated hydrogels, prepared as cylindrical hydrogels specimens with a diameter of 6 mm and height of 2 mm, were incubated at 37°C in PBS. At specific time points, hydrogels were characterized on the basis of compression tests employing a Universal Mechanical Testing Machine (INSTRON 3340) equipped with a load cell of 50 N. The elastic modulus (E) was calculated as the slope of the linear region of the generated stress/strain curve, corresponding to 0-5% strain range (n=3). Hydrogel height was determined using the compression system by lowering down the top plate until contact. To track swelling behaviour as well as the degradation profile of the GA-encapsulated hydrogels in comparison with native laminaran hydrogels, the wet and dry weight was monitored up to 14 days. Thereafter, the hydrogels were removed from the PBS solution and the excess PBS was removed using filter paper. Then the hydrogels were weighed (wet weight) and promptly re-added to PBS to continue the experiment (n=6). For the dry weight, at each time point, hydrogels (n=6) were previously frozen and freeze-dried.

In order to investigate the structure of the hydrogels, Cryo-Scanning Electron Microscopy (Cryo-SEM) analysis was employed, using a High-Resolution Scanning Electron Microscope with X-Ray Microanalysis and Cryo-SEM experimental set-up (JEOL JSM 6301F/ Oxford INCA Energy 350/Gatan Alto 2500). Briefly, hydrogels were frozen and immediately after fractured so their inner structures could be exposed. Then the samples were etched for 120 s at −90 °C, and afterwards coated with Au/Pd by sputtering for 50 s. At the end samples were then transferred into the SEM chamber, and imaged at −150 °C. The measurement of pores' diameter of each sample was performed using ImageJ software. 100 pores for each formulation were randomly selected from different SEM images.

Cell lines and cell cultivation

Human adenocarcinoma alveolar basal epithelial cells (A549, ATCC) were cultured in Ham's F12 Nutrient Medium (Ham's F12, Sigma Aldrich) supplemented with 10% Fetal Bovine Serum (FBS, South American origin, Thermo Fisher Scientific) and 1% antibiotic/antimycotic (Thermo Fisher Scientific). Mesenchymal stem cells (MSCs) were isolated from the Wharton's jelly of human umbilical cords (UC), received from Centro Hospitalar do Baixo Vouga, Aveiro under an established protocol. The samples were collected to a container with PBS supplemented with 1% antibiotic/antimycotic (v/v) and transferred to the laboratory facilities within 24 h after collection and immediately processed. The washing of the UC was performed with sterile PBS several times to remove blood and blood clots. Initially UC was cut into small pieces (3 cm), and the vein and two arteries were removed. Small pieces of the WJ were sliced from the UC and placed separately on adherent petri-dishes The tissues explants were incubated at 37ºC and 5% of CO2 for 2 h with Minimum Essential Medium Alpha (α-MEM, Gibco), supplemented with 1% antibiotic/antimycotic and 10% FBS. The explant cultures were left undisturbed for 5 days to allow the migration of MSCs from the tissues to the petri-dishes. After cell migration, the tissue explants were removed. At 90% confluence, MSCs were detached using 1x trypsin-EDTA (Thermo Fisher Scientific) and seeded in adherent cell culture T-flasks. For both A549 and MSCs, the culture medium was replaced every 2 days and maintained semiconfluent. All cultures were incubated at 37°C in a 5% CO2 high-humidity environment. Evaluation of the efficiency of free glucose resulting from the degradation of laminaran hydrogels to support cell culture. Cells were seeded at a density of 2.7 ×104 (cells/cm2) in 1 mL of full culture media (α-MEM for MSCs and Ham's F12 for A549). After 24 h, cells were treated by replacing the culture medium to DMEM no glucose (Corning), supplemented with 1% antibiotic/antimycotic, 10% FBS, GlutaMax and Sodium Pyruvate (10 mM, Thermofisher), and adding a laminaran hydrogel (40µl,10%

(w/v)) and GA (0, 0.7 and 2% w/v) to the medium of each well. Since glucose concentration is an important factor in sustaining cell growth and viability, selecting the applied enzyme concentration was done according to glucose concentration in the culture medium formulations. Ham's F12 consists of 1.26 mg.mL-1 glucose and α-MEM as a classical culture media for MSCs contains 1mg.mL-1 glucose. Based on sugar analysis results (Figure 2c), by using 0.7% GA in the first 24h, both cells were exposed to relatively similar glucose concentration existing in their typical culture medium and over time they weren't subjected to significantly higher glucose level since in every 72 hours medium was replaced. In order to investigate the impact of higher glucose availability on cell's viability, 2% GA was also tested. Wells containing laminaran hydrogel with no enzyme in full culture medium were used as control samples. Metabolic activity of the treated cells was quantitatively assessed by AlamarBlue fluorescent assay, according to the manufacturer's instructions. At each pre-settled time points, cells were incubated with 10% v/v Alamar Blue (Thermo Fisher Scientific, USA) in warm culture medium for 4 h at 37°C. Then, 100 µL of supernatant were transferred to transparent 96-well plates. Three wells of each condition were analysed, and the fluorescence readings were performed in triplicate. The fluorescence was measured using excitation and emission wavelength of 540 and 600 nm, respectively (Microplate Reader Synergy HTX, Biotek, USA). The viability of control (no enzyme) was regarded as 100%. A Live/dead assay was also performed. At a pre-set time, cells were incubated in a solution of 2 µL of calcein AM solution in DMSO (Thermo Fisher Scientific, USA) and 1 µL of propidium iodide (Thermo Fisher Scientific, USA) in 1000 µL of PBS at 37°C for 15 min. After washing with PBS, cells were observed using a fluorescence microscope (Fluorescence Microscope Zeiss, Axio Imager 2, Zeiss, Germany).

3D cell encapsulation in self-feeding laminaran hydrogel

Cells were encapsulated within the enzyme-immobilized hydrogels, as well as, in native hydrogels and incubated in DMEM no glucose with the same supplements as mentioned before. Native gels incubated in Hams F12 (for A549 cells), and α-MEM (for MSCs) were used as positive controls. For 3D encapsulation, cell suspension was incorporated into the hydrogel precursor solution at a final density of 5x106 cells/mL and cured as described in a previous section. The same GA concentration (0.7% and 2%) were used in the self-feeding hydrogels. According to the previous studies, MSCs have shown remarkable resistance to high level of glucose 40 mM with no impact on proliferation rate.[43] Due to the sugar analysis results (Figure 2d), 0.7% GA encapsulated hydrogels generated less than 40 mM of glucose over 14 days. For this reason, 0.7% GA appears to be the right choice in terms of providing desirable glucose. In addition, 2% GA was tested to explore the reaction of cells to higher glucose concentrations and to investigate the possibility of glucotoxicity. A live/dead assay was performed to visualize the distribution of live and dead cells throughout the hydrogel at different time points. Fluorescence images were taken using a Confocal Microscope (LSM 880, ZEISS). A z-stack with 10 µm step size was acquired per group. These z-stacks were then collapsed to 2D projections to allow quantification of cells viability. Total DNA quantification of the GA-encapsulated hydrogels was performed using a Quant-iT PicoGreen dsDNA kit (Thermo Fisher Scientific, USA). Hydrogels (n = 3) were suspended in ultra-pure sterile water frozen at −80°C and stored until further use. In order to induce disruption of the cells encapsulated in the hydrogels, the samples were thawed at 37°C and placed in an ultrasound bath for ≈30 min. A standard curve for DNA analysis was created based on the DNA standard of the DNA assay kit. After 10 min of incubation at RT, fluorescence was measured at an excitation wavelength of 485 nm and 528 nm of emission using a microplate reader.

In vivo animal studies

Nude mice from both sexes were anesthetized using isoflurane anaesthesia using a controlled vaporizer (1-2% in 0.3 L/min O2 for maintenance and 5% in 1 L/min O2 for induction). Buprenorphine (0.08 mg/kg) (Bupaq, Richter Pharma ag) was given subcutaneously to all animals before surgery. Eye ointment (Siccafluid, Unidoses 2.5 mg/g, Laboratoires THÉA) and heating pad were used during the whole procedure. Surgical asepsis was performed using iodine and alcohol solutions alternated. The surgical procedure consisted of two 0.5 cm incisions performed at the cervical dorsal area and lumbar dorsal area. Three different groups of hydrogels were implanted: self-feeding hydrogels (encapsulating MSCs with 0.7% GA), native cell-laden laminaran hydrogels (encapsulating MSCs without enzyme) and blank hydrogels (without cells and enzyme). All hydrogels were with diameter of 6 mm and height of 3 mm) and were subcutaneously inserted by creating a small dissection tunnel and each incision was closed using 5-0 polyglycolic acid suture line (Surgycril, SMI) and surgical glue (VetBond). Animals were allowed to recover and monitored daily for the rest of the experiment. Paracetamol was maintained in the first 3 days after surgery. Post-surgical analgesia consisted in paracetamol in water (40 mg/ml, Ben-U-Ron, Bene Farmacêutica). Eight samples per condition per time point were implanted into four animals (n = 8 grafts/condition/time point). Animals were anesthetized using isoflurane anesthesia and ultrasounds from the hydrogels were performed using the Vevo 2100 Microultrasound (Fujifilm Visualsonics) at day 1, 7 and 14 to track the shape and size of the hydrogels. Hydrogel's diameters were measured using ImageJ software. The animals were sacrificed at day 7 and day 14 post-implantation using deep isoflurane anaesthesia followed by cervical dislocation. Subsequently, the hydrogels were explanted, and edges of the hydrogels were cut by sharp razor blade (to remove tissue connected parts). Thin slices of the hydrogels (from core of the hydrogels) were promptly stained with Calcein/PI and were observed using a fluorescence microscope (Fluorescence Microscope Zeiss, Axio Imager 2, Zeiss, Germany) to evaluate the cell's viability in vivo. All animal experiments were performed at the i3S animal facility, under the project license number 2021-7. The work performed with animals was reviewed by the internal animal ethics committee and submitted to the competent authority (DGAV) for approval.

Histology Samples were collected by cutting the area around the hydrogel implant to obtain tissue samples including the hydrogel disc in the middle. Samples were fixed in 10% formalin overnight and then embedded in paraffin block. five-µm-thick paraffin-embedded sample sections were coloured with Hematoxylin-Eosin staining (H&E), cell nuclei-blue; cytoplasm, elastin, and collagen-pink). Then, the cross-sections were examined for the quantitative evaluation based on the International Standard (ISO 10993-6, Annex A) criteria by a pathologist. The local effects of the hydrogels were estimated by comparing the tissue response caused by the sham procedure (control). Sham procedure have been done by simply making an incision in the mice skin and opening a pocket under the skin and then closing the wound. At day 7 and 14, mice were sacrificed, and their inflammatory response was explored using H&E slides. Brightfield microscopy was applied to examine pathology of selected samples and control group (at day 7 and day 14), for observing the existence, number, and distribution of polymorphonuclear cells, lymphocytes, plasma cells, macrophages, giant cells, and necrosis. Inflammatory scoring was based on ISO 10993 standard scoring: (scale range of 0.0-2.0 = minimal or no reaction, 3.0-8.9 = slight reaction, 9.0-15.0 = moderate reaction, >15.0= severe reactions).

Statistical analysis was performed using GraphPad Prism software (GraphPad Software Inc., version 8.0) using two-way ANOVA following the Bonferroni post hoc test, with a significance level at $p < 0.01$: *$p < 0.05$; **$p < 0.01$; ***$p < 0.001$; ****$p < 0.0001$. NS indicates no significant difference.

Conflicts of interest

There are no conflicts to declare.

Acknowledgements

This work was developed within the scope of the project CICECO-Aveiro Institute of Materials, UIDB/50011/2020 & UIDP/50011/2020 and LAQV-REQUIMTE (UIDB/50006/2020), financed by national funds through the FCT/MEC and when appropriate co-financed by FEDER under the PT2020 Partnership Agreement and BEAT (PTDC/BTM-MAT/30869/2017). The authors also acknowledge FCT for the project MARGEL (PTDC/BTM-MAT/31498/2017). Mehrzad Zargarzadeh acknowledges the doctoral grant SFRH/BD/143883/2019 and Catarina A. Custódio acknowledges the individual contract CEECIND/02713/2017. Image acquisition was performed by Cátia F. Monteiro in the LiM facility of iBiMED, a node of PPBI (Portuguese Platform of BioImaging): POCI-01-0145-FEDER-022122.

Notes and references

1. A. Khademhosseini and R. Langer, *Biomaterials*, 2007, **28**, 5087-5092.
2. L. W. Chow and J. F. Fischer, *Exp Biol Med (Maywood)*, 2016, **241**, 1025-1032.
3. C. R. Correia, S. Nadine and J. F. Mano, *Adv. Funct. Mater*, 2020, **30**, 1908061.
4. C. D. Spicer, *Polymer Chemistry*, 2020, **11**, 184-219.
5. E. M. Ahmed, *Journal of Advanced Research*, 2015, **6**, 105-121.
6. Q. Chai, Y. Jiao and X. Yu, *Gels*, 2017, **3**, 6.
7. J. F. Mano, G. A. Silva, H. S. Azevedo, P. B. Malafaya, R. A. Sousa, S. S. Silva, L. F. Boesel, J. M. Oliveira, T. C. Santos, A. P. Marques, N. M. Neves and R. L. Reis, *J. R. Soc. Interface*, 2007, **4**, 999-1030.
8. R. Mohammadinejad, H. Maleki, E. Larrañeta, A. R. Fajardo, A. B. Nik, A. Shavandi, A. Sheikhi, M. Ghorbanpour, M. Farokhi, P. Govindh, E. Cabane, S. Azizi, A. R. Aref, M. Mozafari, M. Mehrali, S. Thomas, J. F. Mano, Y. K. Mishra and V. K. Thakur, *Applied Materials Today*, 2019, **16**, 213-246.
9. E. Jabbari, J. Leijten, Q. Xu and A. Khademhosseini, *Materials Today*, 2016, **19**, 190-196.
10. M. B. Oliveira, H. X. S. Bastos and J. F. Mano, *Biomacromolecules*, 2018, **19**, 2742-2749.
11. S. Azevedo, A. M. S. Costa, A. Andersen, I. S. Choi, H. Birkedal and J. F. Mano, *Advanced materials (Deerfield Beach, Fla.)*, 2017, **29**.
12. S. U. Kadam, B. K. Tiwari and C. P. O'Donnell, *Int J Food Sci Technol*, 2015, **50**, 24-31.
13. M. Zargarzadeh, A. J. R. Amaral, C. A. Custódio and J. F. Mano, *Carbohydrate Polymers*, 2020, **232**, 115774.
14. A. M. S. Costa, J. M. M. Rodrigues, M. M. Pérez-Madrigal, A. P. Dove and J. F. Mano, *Journal of the American Chemical Society*, 2020, DOI: 10.1021/jacs.0c09489.
15. C. R. Martins, Custódio, C.A. , Mano, J.F., *Carbohydrate Polymers* 2018, **202**, 91–98.
16. R. R. Remya, S. R. R. Rajasree, T. Y. Suman, L. Aranganathan, S. Gayathri, M. Gobalakrishnan and M. G. Karthih, *Materials Research Express*, 2018, **5**, 035403.
17. C. A. Custódio, R. L. Reis and J. F. Mano, *Biomacromolecules*, 2016, **17**, 1602-1609.
18. T. Rademakers, J. M. Horvath, C. A. van Blitterswijk and V. L. S. LaPointe, *Journal of Tissue Engineering and Regenerative Medicine*, 2019, **13**, 1815-1829.
19. J. Rouwkema, B. F. J. M. Koopman, C. A. V. Blitterswijk, W. J. A. Dhert and J. Malda, *Biotechnology and Genetic Engineering Reviews*, 2009, **26**, 163-178.
20. G. Yang, B. Mahadik, J. Y. Choi and J. P. Fisher, *Progress in Biomedical Engineering*, 2020, **2**, 012002.
21. D. Lei, Y. Yang, Z. Liu, B. Yang, W. Gong, S. Chen, S. Wang, L. Sun, B. Song, H. Xuan, X. Mo, B. Sun, S. Li, Q. Yang, S. Huang, S. Chen, Y. Ma, W. Liu, C. He, B. Zhu, E. M. Jeffries, F.-L. Qing, X. Ye, Q. Zhao and Z. You, *Materials Horizons*, 2019, **6**, 1197-1206.
22. M. D. Sarker, S. Naghieh, N. K. Sharma and X. Chen, *Journal of Pharmaceutical Analysis*, 2018, **8**, 277-296.
23. V. M. Gaspar, P. Lavrador, J. Borges, M. B. Oliveira and J. F. Mano, *Mater. Horiz*, 2020, **32**, 1903975.
24. P. A. Shiekh, A. Singh and A. Kumar, *ACS Applied Materials & Interfaces*, 2018, **10**, 18458-18469.
25. S. Suvarnapathaki, X. Wu, D. Lantigua, M. A. Nguyen and G. Camci-Unal, *NPG Asia Materials*, 2019, **11**, 65.
26. M. Deschepper, K. Oudina, B. David, V. Myrtil, C. Collet, M. Bensidhoum, D. Logeart-Avramoglou and H. Petite, *Journal of Cellular and Molecular Medicine*, 2011, **15**, 1505-1514.

27. A. Moya, J. Paquet, M. Deschepper, N. Larochette, K. Oudina, C. Denoeud, M. Bensidhoum, D. Logeart-Avramoglou and H. Petite, *STEM CELLS*, 2018, **36**, 363-376.
28. H. N. Cheng and Q.-M. Gu, *Polymers*, 2012, **4**.
29. D. Wang, D. H. Kim, N. Seo, E. J. Yun, H. J. An, J.-H. Kim and K. H. Kim, *Applied and Environmental Microbiology*, 2016, **82**, 4340-4349.
30. D. H. Kim, D. H. Kim, S.-H. Lee and K. H. Kim, *Biotechnology for Biofuels*, 2018, **11**, 64.
31. F. C. Pavezzi, E. Gomes and R. da Silva, *Braz J Microbiol*, 2008, **39**, 108-114.
32. P. Kumar and T. Satyanarayana, *Critical Reviews in Biotechnology*, 2009, **29**, 225-255.
33. S. Ermakova, R. Men'shova, O. Vishchuk, S.-M. Kim, B.-H. Um, V. Isakov and T. Zvyagintseva, *Algal Research*, 2013, **2**, 51-58.
34. S. K. Vashist, E. Lam, S. Hrapovic, K. B. Male and J. H. T. Luong, *Chemical Reviews*, 2014, **114**, 11083-11130.
35. Z.-K. Cui, S. Kim, J. J. Baljon, B. M. Wu, T. Aghaloo and M. Lee, *Nature Communications*, 2019, **10**, 3523.
36. H. Zhao, L. Li, S. Ding, C. Liu and J. Ai, *Materials Letters*, 2018, **223**, 21-24.
37. S. M. LaNasa, I. T. Hoffecker and S. J. Bryant, *J. Biomed. Mater. Res.*, 2011, **96B**, 294-302.
38. A. Lueckgen, D. S. Garske, A. Ellinghaus, D. J. Mooney, G. N. Duda and A. Cipitria, *Biomaterials*, 2019, **217**, 119294.
39. A. B. Blakeney, P. J. Harris, R. J. Henry and B. A. Stone, *Carbohydrate Research*, 1983, **113**, 291-299.
40. D. Schop, F. W. Janssen, L. D. van Rijn, H. Fernandes, R. M. Bloem, J. D. de Bruijn and R. van Dijkhuizen-Radersma, *Tissue Eng Part A*, 2009, **15**, 1877-1886.
41. C. Devillé, J. Damas, P. Forget, G. Dandrifosse and O. Peulen, *Journal of the Science of Food and Agriculture*, 2004, **84**, 1030-1038.
42. International Organization for Standardization, https://www.iso.org/standard/61089.html, (accessed December 2016).
43. Y.-M. Li, T. Schilling, P. Benisch, S. Zeck, J. Meissner-Weigl, D. Schneider, C. Limbert, J. Seufert, M. Kassem, N. Schütze, F. Jakob and R. Ebert, *Biochemical and Biophysical Research Communications*, 2007, **363**, 209-215.